Comparative Analysis of Numerical Methods for the Neural Field Equation

Alexandre Cabral
alexandre.cabral@ist.utl.pt

Instituto Superior Técnico, Lisboa, Portugal

May 2022

Abstract

The number of neurons and synapses that exist in a small patch of cortex is immense. The Neural Field Equations (NFE) constitute an essential tool in the analysis of the behavioral dynamics of these neuron populations. The neuronal field models represent, on a large scale, the spatial dynamics of networks of neurons in terms of nonlinear integro-differential equations. These equations describe the space-time evolution of variables such as membrane potentials or activity at synapses. They play an important role in various fields such as Robotics, mainly in the creation of autonomous robots that interact with other agents to jointly solve a task. Therefore, simulations play an important role in the study of brain dynamics. This work analyzes one-dimensional deterministic NFEs, taking into account the delays caused by finite transmission speed and external stimulus, and presents several numerical methods to solve them, which are studied for their convergence and complexity. In a second phase, these methods are used to study working memory and the conditions under which this phenomenon occurs. To conclude, we present some simulations that illustrate the various steps of how the working memory effect in the brain is processed. MatLab is used as the programming language that implements the algorithm, in order to simulate the neural fields studied in this paper.
Keywords: Deterministic neural field equations, finite transmission speed, external stimulus, working memory, MatLab

1. Introduction

1.1. Motivation

One of the main challenges in neuroscience is to understand how neuronal mechanisms such as learning, attention, cognition, long term memories, are formed in the brain. All of these mechanisms listed above share one thing - memory or working memory. For example, learning is a process by which we integrate new knowledge generated as a result of experiences. The product of such experiences is converted into memories stored in our brain. To understand this phenomenon on we have to give first the beginnings of mathematical models for neuroscience. In 1952, A.H. Hodgkin and A.F. Huxley, see [2], wrote a paper describing how action potentials in neurons are initiated and propagated, using the language of electrical circuits and translating them into a system of four ordinary differential equations. Further investigation of nerve stimulus propagation led in 1962 to the FitzHugh-Nagumo equations, [3], [4], [5], where the Hodgkin-Huxley system is reduced to two equations that describe the propagation of impulses in the nervous system. However, these classical neuroscience models were not applicable to a large population of nerve cells. The real human brain contains about 100 billion neurons with roughly 10^{14} synapses between them. A human's cerebral cortex is about 2-4 millimeters thick and contains about a fifth of all neurons. According to recent estimates, the cortex can store up to 100 Tb (1014 bytes) of data. This large number of neurons and synapses distributed along such limited region, lead us to treat the cortex as a virtually continuum space. Due to its small thickness, the cortex (or its parts) are often considered as one- or two-dimensional domains. To surpass the dificulties of dealing with such amount of nerve cells Wilson and Cowan [9] and Amari [10], in the 1970's, developed a continuous neural field approach to model the brain areas with high neuronal density. Originally, the Neural Field Equation (NFE) derived by Amari describes the average membrane potential of the neurons located at x at instant t, $V(x,t)$. Here, we analyse the equation in the one-dimensional case:

$$\frac{\partial}{\partial t}V(x,t) = S(x,t) - \alpha V(x,t) + \int_\Omega K(|x-y|)f(V(y,t))dy \quad (1)$$

where $V(x,t)$ is a continuous unknown function $V : \Omega \times [0,T] \to \mathbb{R}$ and represents the neuronal membrane potential at point x and instant t.

$S(x,t)$ represents an external excitation source (stimulus) and f the firing rate of neurons, that is, the ability of the neuron to emit a signal as a function of the membrane potential.

$K(|x-y|)$ is a connectivity function and represents the strength of the interaction between neurons at positions x and y. It is assumed that K depends only on the distance between x and y.

α is a constant that represents the rate of decrease of potential, resulting from dissipation.

Ω represents the considered domain.

2. Numerical methods

2.1. Discretization

To numerically treat the equation (1), within the time interval $[0,T]$, we define a step τ and a network of points $t_j = j\tau$, $j = 0, 1, ..., n_t$.
In the range $\Omega = [-L, L]$ in space, we define a step h and a point lattice $x_i = -L + ih$, $i = 0, 1, ..., N$.
We will use three methods, one explicit, one semi-implicit and finally, one fully implicit. The partial derivative with respect to time of the potential $V(x,t)$ is treated using a forward difference, in the case of the explicit Euler method, and backward, in the case of the semi-implicit and implicit ones. We rewrite (1) equation as follows:

$$\frac{\partial}{\partial t}V(x,t) = S(x,t) - \alpha V(x,t) + \kappa(V(x,t))$$

$$t \in [0,T], x \in \Omega \subset \mathbb{R} \quad (2)$$

$$V(x,0) = V_0(x),$$

where κ denotes the non linear integral operator defined by

$$\kappa(V(x,t)) = \int_\Omega K|x-y|f(V(y,t-r(x,y)))dy \quad (3)$$

2.2. Explicit method

The forward Euler method for (2) appears in the following way:

$$\frac{V_{i,j+1} - V_{i,j}}{\tau} = S_{i,j} - \alpha V_{i,j} + \kappa_{i,j}, \quad i = 0, ..., N, \quad j = 0, ..., n_t - 1 \quad (4)$$

where

- $V_{i,j}$ represents the aproximation of $V(x_i, t_j)$
- $S_{i,j}$ represents $S(x_i, t_j)$
- $\kappa_{i,j}$ represents the aproximation of the integral in the right hand side of (1)

2.3. Semi-Implicit method

We present here a semi-implicit method in time that calculates the external stimulus $S(x,t)$ and the solution $V(x,t)$ at point $(i, j+1)$ in the network.

The semi-implicit Euler method is presented as follows:

$$\frac{V_{i,j+1} - V_{i,j}}{\tau} = S_{i,j} - \alpha V_{i,j+1} + \kappa_{i,j}, \quad i = 0, ..., N, \quad j = 0, ..., n_t - 1 \quad (5)$$

becoming

$$V_{i,j+1} = \frac{\tau(S_{i,j} + \kappa_{i,j}) + V_{i,j}}{1 + \alpha\tau} \quad (6)$$

2.4. Implicit method

The method consists of the following

$$\frac{V_{i,j+1} - V_{i,j}}{\tau} = S_{i,j+1} - \alpha V_{i,j+1} + \kappa_{i,j+1} \quad (7)$$

where the difference from the previous method is the calculation of the integral in time step $j+1$, as in the case of the other parameters.

Differently from the explicit and semi-implicit methods, with this algorithm at each time step we have to solve a system of nonlinear equations.

To solve this system, we use the fixed point method. We will show that, under certain conditions, at each time step, the system of equations (7) has a solution and that this solution can be approximated by the fixed point method. We will use reasoning similar to what was used in [13].

2.5. Convergence of the Implicit Method

We use, in the following, this definition

$$V_j(x) = V(x, t_j) \quad \forall x \in \Omega, \quad i = 0, ..., n.$$

We represent by $U_j(x)$ the aproximated solution of equation (2) in time step t_j. To approximate the derivative of V with respect to time, we use the difference:

$$\frac{\partial}{\partial t}U(x,t_j) \approx \frac{U_{j+1}(x) - U_j(x)}{\tau} \quad (8)$$

Substituting the equation (8) into equation (2) we get

$$\frac{U_{j+1}(x)-U_j(x)}{\tau} = S_{j+1} - \alpha U_{j+1}(x) + \kappa_{j+1}(U_{j+1}(x)) \quad j=0,...,n-1 \tag{9}$$

The equation (9) can be rewritten in the following way

$$U_{j+1}(x) - \frac{1}{\alpha+\frac{1}{\tau}}\kappa(U_{j+1}(x)) = f_{j+1}(x), \quad x\in\Omega \tag{10}$$

where

$$f_{j+1}(x) = \Big(\alpha+\frac{1}{\tau}\Big)^{-1}\Big(S_{j+1}+\frac{U_j(x)}{\tau}\Big), \quad x\in\Omega \tag{11}$$

Equations (10)-(11) define a nonlinear Fredholm integral equation of the second kind and we will analyse its solvability using standard results of functional analysis. In order to apply the Banach fixed point theorem, we define the iterative process:

$$U_{j+1}^{(\gamma)} = \lambda\kappa(U_{j+1}^{(\gamma-1)}) + f_{j+1}(x) = G(U_{j+1}^{\gamma-1}), \quad x\in\Omega, \quad \gamma=1,2,... \tag{12}$$

where

$$\lambda = \frac{1}{\alpha+\frac{1}{\tau}} = \frac{\tau}{1+\alpha\tau} \tag{13}$$

If the function G is contractive in a certain closed set $X\subset C([-L,L])$, such that $G(X)\subset X$, then by the Banach fixed point theorem, equation (10) has a unique solution in X and the sequence $U_{j+1}^{(\gamma)}$ defined by (12), converges to this solution in the maximum norm. The sequence converges for any initial guess $U_{j+1}^{(0)}\in X$. In our case, the solution is by construction the iterate U_{j+1}, that is close to U_j. Therefore it makes sense to assume X is a certain closed set which contains U_j and choose $U_{j+1}^{(0)}=U_j$. To prove that G is contractive in X we need to show that for a certain constant L, $L<1$, we have

$$||G(V)-G(U)||_\infty \le L||V-U||_\infty, \quad \forall U,V \in X \tag{14}$$

where the norm is the maximum norm in $C([-L,L])$.

From formula (12)

$$||G(V)-G(U)||_\infty \le \lambda\int_\Omega |K(x-y)||f(V)-f(U)|dy \tag{15}$$

Using the mean value theorem for integrals, we get

$$||G(V)-G(U)||_\infty \le \lambda|\Omega|.||K||_\infty \max_{U,V\in X}|f(V)-f(U)| \tag{16}$$

where $|\Omega|$ denotes the length of Ω. Assuminng that the firing rare f has a bounded continuous derivative in $\mathbb{R}$, we can write:

$$||G(V)-G(U)||_\infty \le \lambda|\Omega|.||K||_\infty f_{max}||V-U||_\infty \tag{17}$$

where

$$f_{max} = \max_{x\in\mathbb{R}}|f'(x)|. \tag{18}$$

Hence, (14) is satisfied with

$$L = \lambda|\Omega|.||K||_\infty f_{max} \tag{19}$$

Recall that

$$\lambda = \frac{\tau}{1+\alpha\tau} < \tau. \tag{20}$$

Therefore, in order to satisfy $L<1$ it is sufficient to require that

$$\tau|\Omega|.||K||_\infty f_{max} < 1 \tag{21}$$

or equivalently

$$\tau < \frac{1}{|\Omega|.||K||_\infty f_{max}} \tag{22}$$

From (22) we conclude that G will be contractive in a certain set $X\subset[-L,L]$ if we take τ sufficiently small and then we show that the fixed point method converges. Then the iterative process in (12) with $U_{j+1}^{(0)}=U_j$ converges to the solution of (10).

The system (7) results from discretizing (10) in space, using the trapezium rule. Therefore, it is necessary to show that, using the discretization, the fixed point theorem is reapplicable. We use an argument similar to the one used in section 2.1.2. of [13].

When we introduce the trapezzium rule for the calculation of the integral $\kappa(U)$, we introduce a finite aproximation for the integral operator κ. Consider U^h the vector with $N+1$ entries such that:

$$(U^h)_i = U(x_i), \quad i=0,1,N$$

Then, the finite aproximation of κ can be given by:

$$(\kappa^h(U^h))_m = h\Big(\frac{g_1(x_0)+g_1(x_N)}{2} + \sum_{k=1}^{N-1} g_1(x_k)\Big) \tag{23}$$

with

$$g_1(x_k) = K(|x_m - x_k|)f((U^h)_k) \qquad m = 0, 1, ..., N \tag{24}$$

Substituting κ by κ^h in equation (10), it turns:

$$(U^h)_i - \frac{1}{\alpha + \frac{1}{\tau}}(\kappa^h(U^h))_i = (f^h)_i, \qquad i = 0, 1, ..., N \tag{25}$$

where $\kappa^h(U^h)$ is defined by (23) and

$$(f^h)_i = f(x_i), \qquad i = 0, 1, ..., N \tag{26}$$

with f defined by (11).

Note that system (25) is equivalent to system (7), which defines the implicit Euler method for the considered equation.

To calculate $(f^h)_i$ in instant $j+1$ we have to calculate U_j in that specific point of Ω_h. Therefore, in each time step of our method, we have to solve (25), which is a system with $N+1$ non linear equations.

Consider the iterative process

$$U^{h,(\gamma)} = \lambda\kappa(U^{h,(\gamma-1)}) + f^h(x) = G^h(U^{h,(\gamma-1)}), \qquad \gamma = 1, 2, ... \tag{27}$$

As in case of Fredholm integral equation, the convergence of the iterative process (27) depends on the contractivity of G^h.

Using the same arguments as before, by analogy with (17), we obtain

$$||G^h(V) - G^h(U)||_\infty \leq \lambda K_{max} f_{max} ||V - U||_\infty Nh$$
$$\leq \lambda K_{max} f_{max} ||V - U||_\infty |\Omega| \tag{28}$$

for $U, V \in X^h \subset \mathbb{R}^{N+1}$ where:

$$K_{max} = \max_{x_m, y_i \in \Omega_h} |K(|x_m - y_i|)| \tag{29}$$

It follows that that the function G^h is Lipschitzian in X^h with constant L_1

$$L_1 = \lambda K_{max} f_{max} |\Omega| \tag{30}$$

where λ is defined by (13).

The equality (30) is identical to (19), with the difference that the norm $||K||$ is substituted by K_{max}. Therefore, repeating the argument expressed by the formulas (20) and (21), we get the formula, similar to (22):

$$\tau < \frac{1}{K_{max} f_{max} |\Omega|} \tag{31}$$

We conclude that, if τ satisfies inequation (31) above, then the non linear equation (25) has a unique solution $U^h \in X^h$, where $X^h \subset \mathbb{R}^{N+1}$ is a certain closed set which contains U_j^h. Moreover, the iterative process defined by (27) with $U^{h,(0)} = U_j^h$ converges to this solution. The problem that emerges is the one of the convergence U^h to U_j when $h \to 0$. To analyze this question, we solve equation (10) in each point of the network Ω_h.

$$U_{j+1}(x_i) - \frac{1}{\alpha + \frac{1}{\tau}}\kappa(U_{j+1}(x_i)) = f_{j+1}(x_i), \qquad x \in \Omega_h \tag{32}$$

Subtracting equation (25) to (32):

$$U_{j+1}(x_i) - U_i^h = \lambda(\kappa(U_{j+1}(x_i)) - \kappa^h(U_i^h)), \qquad i = 0, 1, ..., N \tag{33}$$

Note that

$$\kappa(U_{j+1}(x_i)) - \kappa^h(U_i^h) = \Big(\kappa(U_{j+1}(x_i)) - \kappa^h(U_{j+1}(x_i))\Big) + \Big(\kappa^h(U_{j+1}(x_i)) - \kappa^h(U_i^h)\Big) \tag{34}$$

Substituting (34) in (33) results

$$U_{j+1}(x_i) - U_i^h = \lambda\Big(\kappa(U_{j+1}(x_i)) - \kappa^h(U_{j+1}(x_i)) + \kappa^h(U_{j+1}(x_i)) - \kappa^h(U_i^h)\Big), \qquad i = 0, 1, ..., N \tag{35}$$

From (35) we obtain

$$||U_{j+1} - U^h||_\infty \leq \lambda\Big(||\kappa(U_{j+1}) - \kappa^h(U_{j+1})||_\infty + ||\kappa^h(U_{j+1}) - \kappa^h(U^h)||_\infty\Big) \tag{36}$$

The second term in the last sum can be writen in terms of $||U_{j+1} - U^h||$ if we know that κ^h is a Lipschitz function, exists a constante L_1 such that

$$||\kappa^h(U_{j+1}) - \kappa^h(U^h)||_\infty \leq L_1 ||U_{j+1} - U^h||_\infty, \qquad \forall U_{j+1}, U^h \in X^h \tag{37}$$

where L_1 is given by (30).

This way, we can rewrite (36) in the form:

$$||U_{j+1} - U^h||_\infty(1 - \lambda L_1) \leq \lambda(||\kappa(U_{j+1}) - \kappa^h(U_{j+1})||_\infty) \quad (38)$$

From (20), we have $\lambda < \tau$ and we obtain $\lambda L_1 < 1$ if τ satisfies condition (31).

Finally, to calculate $||\kappa(U_{j+1}) - \kappa^h(U_{j+1})||_\infty$, we should recall that κ_h is obtained by applying the trapezium rule with step h. Then, if U_{j+1},K and S are sufficiently smooth, there exists a certain $M > 0$, which does not depend on h such that:

$$||\kappa(U_{j+1}) - \kappa^h(U_{j+1})||_\infty \leq Mh^2 \quad (39)$$

From (38) and (39) we conclude that there exists a constant M_1 such that

$$||U_{j+1} - U^h||_\infty \leq M_1 h^2 \quad (40)$$

Finally, the following bound for the error verifies

$$||U_{j+1} - U^h||_\infty = O(h^2), \qquad h \to 0. \quad (41)$$

and we get second order convergence in order to space step h in the implicit method.

The convergence of the semi-implicit method can be proved using arguments similar to those used in [12]. In the case of the explicit method, it can be proved that it is convergent if $\zeta < \alpha$ and τ verifies

$$\tau < \frac{2}{\alpha - \zeta} \quad (42)$$

where $\zeta = \|f\|_\infty \|K\|_\infty$.

3. Numerical Examples

We introduce here four examples to illustrate the performance of the methods described above. The solutions of the first two examples are only time dependent. The solutions of the other two are dependent in time and space.

3.1. Example 1

We introduce here a first example already used in [13] in which the exact solution is only time dependent,

$$K(|x - y|) = e^{-(x-y)^2}$$

$$S(x,t) = -\tanh(\sigma \exp(\frac{-t}{c}))b(x,y) \quad (43)$$

$$f(x) = \tanh(x)$$

where $b(x) = \int_{-1}^{1} K(x,y)dy = \frac{\sqrt{\pi}}{2}(Erf(1+x) + Erf(1-x))$.

The initial condition is given by $V_0(x) = 1$

The exact solution of this example is:

$$V(x,t) = \exp(-t)$$

We present below the tables with the errors and orders of convergence with respect to τ for the three methods, explicit, semi-implicit and implicit in the time interval $t \in [0,1]$ and space interval $x \in [-1,1]$ with a step size $h = 0.1$.

To test the order of convergence z with respect to time step τ, or h we use the following formula which calculates the error e_τ with the maximum norm:

$$e_{h,\tau} = \max_{i=0,1,\ldots,N} |V(x_i,t_n) - V_{i,n}|$$

$$z_\tau = \frac{\log \frac{e_{h,\tau/2}}{e_{h,\tau}}}{\log \frac{1}{2}}, \quad z_h = \frac{\log \frac{e_{h/2,\tau}}{e_{h,\tau}}}{\log \frac{1}{2}} \quad (44)$$

τ	$e_{h,\tau}$	z_τ
0.001	0.00033844	0.9868
0.002	0.00067071	0.99362
0.004	0.0013355	0.99733

Table 1: Error and order of Convergence for the explicit method

τ	$e_{h,\tau}$	z_τ
0.001	0.00062232	0.9999
0.002	0.0012446	0.99743
0.004	0.0024847	0.99371

Table 2: Error and order of Convergence for the semi-implicit method

τ	$e_{h,\tau}$	z_τ
0.001	0.00026862	1.0034
0.002	0.0005385	1.0012
0.004	0.0010779	0.99969

Table 3: Error and order of Convergence for the implicit method

Analyzing the values in the tables, we conclude that the implicit method provides the best results, with the smallest error value. In the comparison between explicit and semi-implicit, the explicit presents a smaller error. In any of the three methods, the estimate of the order of convergence is close to 1, which is in agreement with the well-known properties of the Euler method.

3.2. Example 2

We now consider an example where the solution is increasing with time.

$$K(|x-y|) = \exp(-(x-y)^2)$$

$$f(x) = \tanh(x)$$

$$S(x,t) = 1 + t - \tanh(t)b(x,y)$$

where $b(x) = \int_{-1}^{1} K(x,y)dy = \frac{\sqrt{\pi}}{2}(Erf(1+x) + Erf(1-x))$

The initial condition is given by $V_0(x) = 0$

The exact solution of this example is:

$$V(x,t) = t$$

We now present the errors and orders of convergence with respect to the step in space, h, for the three methods, explicit, semi-implicit and implicit for the interval $t = [0, 0.1]$ and an interval in space $[-1.1]$ with a step $\tau = 0.001$.

h	$e_{h,\tau}$	z_h
0.05	3.6013e-05	2.0002
0.1	0.00014407	2.0008
0.2	0.00057663	1.9474

Table 4: Error and order of Convergence for the explicit method

h	$e_{h,\tau}$	z_h
0.05	0.00015259	0.042411
0.1	0.00015715	0.15835
0.2	0.00017538	0.46333

Table 5: Error and order of Convergence for the semi-implicit method

h	$e_{h,\tau}$	z_h
0.05	1.5515e-06	2.0003
0.1	6.2075e-06	2.0013
0.2	2.4853e-05	1.9472

Table 6: Error and order of Convergence for the implicit method

The values in the tables indicate a smaller error in the implicit method, followed by the explicit and finally the semi-implicit method. In this example, the error norm for the semi-implicit method is much higher than for any of the other methods. In this method, the error decreases very slowly when decreasing h. This results from the fact that in this method (contrary to what happens in the others), the error resulting from discretization in time has a greater weight than that resulting from discretization in space. Thus, when h is decreased, the error decreases, but this is not reflected in the estimate of the order of convergence, which does not reflect the actual order of convergence of the method.

3.3. Example 3

Here we present an example where the solution depends on a certain parameter α. For certain values of α, the solution never reaches the critical value of the firing rate. In this case, the solution does not depend on x (it only depends on t). For other values of α, the solution reaches the critical value. In this case, the second-hand integral is no longer null and the solution also depends on x.

The integro-differential equation is presented as follows

$$\frac{\partial}{\partial t}V(x,t) = -\alpha V(x,t) + \exp(-\alpha t) + \int_{\Omega} K(|x-y|)f(V(y,t))dy \tag{45}$$

with $\alpha \in \mathbb{R}^+$,

$$K(x) = \exp(-x^2) \tag{46}$$

$$f(v) = \begin{cases} 0, & \text{if} \quad v < \theta \\ 1, & \text{if} \quad v \geq \theta \end{cases} \tag{47}$$

where $\theta = 0.5$.

Supposing an initial condition $V(x,0) = V_0 < \theta$, the solution of (45) is

$$V(x,t) = c\exp(-\alpha t) + t\exp(-\alpha t) \tag{48}$$

where c is a constant which verifies $c = V_0$.

We present two figures of the different solutions we obtain depending on the value of α, the first for $\alpha = 1$ and the second for $\alpha = 0.5$.

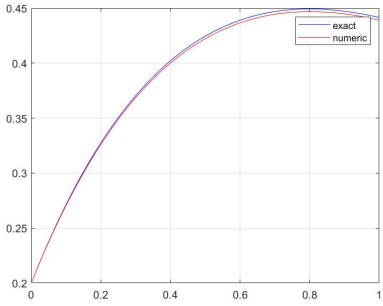

Figure 1: Exact and numeric solution for $\alpha = 1$, with $\tau = 0.01$, $h = 0.05$ and $V(x, 0) = 0.2$

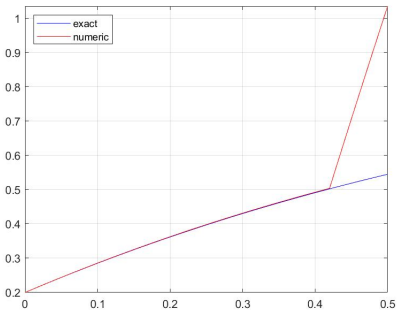

Figure 2: Exact solution (48) and numerical solution for $\alpha = 0.5$, with $\tau = 0.01$, $h = 0.05$ and $V(x, 0) = 0.2$

In Figure 1 is represented the exact and approximated solution, in the case of $\alpha = 1$. As can be seen by the graphic, in this case we have $V(x, t) < 0.5$, for $t \in [0, 1]$ and the solution is given by (48).

In Figure 2 when $t = 0.415$, the solution $V(x, t)$ hits the value 0.5 and the integral in equation (45) is no longer null, therefore the solution is not given by (48) as in the case of $\alpha = 1$.

3.4. Example 4

Finally, we introduce a new example where $S(x, t)$=0, in which a closed form is known for the stationary solution of the problem.

The integro-differential equation is presented as follows:

$$\frac{\partial}{\partial t}V(x,t) = -\alpha V(x,t) + \int_{\Omega} K(x-y)f(V(y,t))dy \tag{49}$$

with $\alpha \in \mathbb{R}^+$,

where f is defined by (47), with $\theta = 0$.

Suppose that

$$K(x) = 3.5e^{-1.8|x|} - 3e^{-1.52|x|} \tag{50}$$

Define

$$W(x) = \begin{cases} \dfrac{x}{|x|}[1.94(1 - e^{-1.8|x|}) \\ +1.97(e^{-1.52|x|} - 1)], & \text{if} \quad x \in \mathbb{R} \setminus \{0\} \\ \\ 0, & \text{if} \quad x = 0 \end{cases} \tag{51}$$

The function W is an odd function and as it can be shown in this case equation (49) has a stationary solution of the form:

So,

$$V(x) = W(x) - W(x - 2.287978) \tag{52}$$

Then, $V(x) > 0$ if and only if $x \in [0, a]$.

Regardless of the initial approximation, the solution of the equation (49) tends towards the stationary solution (52) as t approaches infinity.

Here we consider $V_0(x) = V(x)$ as the initial condition, we obtain the following table which illustrates the error and order of convergence in space step h for the stationary solution using the implicit Euler method with $\tau = 0.001$ and a space interval $[-3, 3]$ with time interval $t = [0, 10]$.

h	$e_{h,\tau}$	z_h
0.025	0.0053414	1.0255
0.05	0.010873	0.97564
0.1	0.021382	1.0381

Table 7: Error and order of Convergence for the implicit method

Analyzing table 7, we see that the error of the method decreases linearly with decreasing the step in space h, contrary to the order 2 that would be expected using the trapezium method for solving the integral. This happens because the integrand function is not differentiable, which is due to the fact that we are using the Heaviside function as the firing rate f, which is not continuous at $x = 0$.

To solve this and obtain a differentiable integrand function, we use a known continuous approximation of the Heaviside function:

$$f_1(x) = \frac{1}{1 + e^{-kx}} \tag{53}$$

for some large k.

After this change in the firing rate function, we obtained the following orders of convergence illustrated by the table 8

h	z_h
0.025	2.4048
0.05	2.0707
0.1	2.4902

Table 8: Error and Order of Convergence using function f_1 as firing rate with $k = 180$

Comparing with table 7, replacement of the Heaviside function by a continuous function caused an increase in the order of convergence to values close to 2, as would be expected. This change canceled the deceleration that was being caused to the method by the discontinuity of the Heaviside function at the point $x = 0$.

4. Simulation of Working Memory

In this chapter we will apply the numerical methods studied in chapter 2 to some NFE cases that were studied in [14] and which are related to working memory modeling. Given a transient external excitation $S(x,t)$, we compare its effect on neuronal potential, during and after the period in which it is active.

To study this case, we have the general NFE equation (1) with a parameter $\theta > 0$ where it is the value to which the neuronal field activity converges in the absence of external stimulation.

$$\frac{\partial}{\partial t}V(x,t) = S(x,t) - \alpha V(x,t) + \int_{\mathbb{R}} K(|x-y|)f(V(y,t))dy - \theta \qquad (54)$$

$$V(x,0) = V_0(x)$$

The connectivity function K has the form,

$$K(x,y) = Ae^{-k|x-y|}(k\ sin(|bx|) + cos(bx)) \qquad (55)$$

where $A > 0$ and $0 < b \leq 1$ control the amplitude and the zero crossings, respectively.

k controls the rate at which the oscillations of the K function decay with distance.

The function $S(x,t)$ that represents the stimulation is of the Gaussian type and is defined in such a way that, from a certain instant t_i, $S(x,t)$ becomes constant.

$$S(x) = (S_s\ e^{-x^2/(2\sigma^2)} - S_i) \qquad (56)$$

$$S(x,t) = \begin{cases} S(x) & t < t_i \\ 0 & t \geq t_i \end{cases} \qquad (57)$$

After this moment $t = t_i$, starts the important part of the process, from the point of view of the applications. In the absence of external stimulus, we will see if the solution is altered or if it remains as if no signal had occurred. In order to simulate neuronal activity, we performed several tests illustrated in the following figures. The external signal variables have the values $S_s = 8$ and $S_i = 0.5$.
The values of σ considered were $0.4; 3; 13$.

4.1. Solution with $\sigma = 0.4$

In the case of $\sigma = 0.4$ the solution over time for $x = 0$ is represented in Fig.3. From the shape of the graph it is clear that at the instant $t = 10$, there is no longer external stimulus. Therefore, the solution increases until $t = 10$ and then decreases. From $t = 15$, the graph of the solution practically coincides with that of the stationary solution, to which it converges when $t \to \infty$.

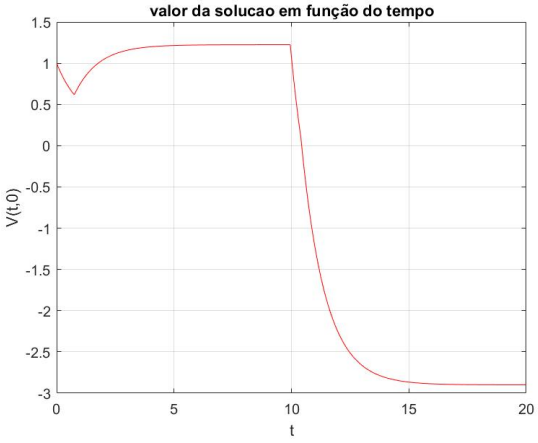

Figure 3: Solution in $x = 0$ as a function of time in case of $\sigma = 0.4$

In Fig.4, the external stimulus and the solution, at $t = 10$, are represented in red and blue, respectively. As we can see the solution behaves similarly to the external signal. The stimulus shapes the form of the figure while $t \leq 10$.

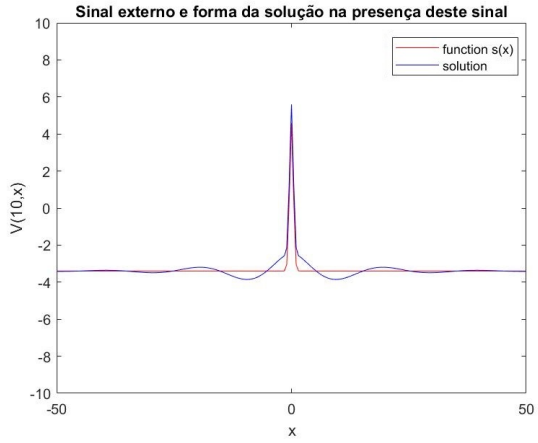

Figure 4: External stimulus and solution in $t = 10$ in case of $\sigma = 0.4$

When representing the solution in $t = 20$, we see that the stimulus was not strong enough to create a "memory effect" in the neurons. The final solution is constant equal to the value of θ. This happens because the external signal $S(x)$ was not "strong

enough". The value of σ was still low, to create a change in the neuronal field and create the memory effect.

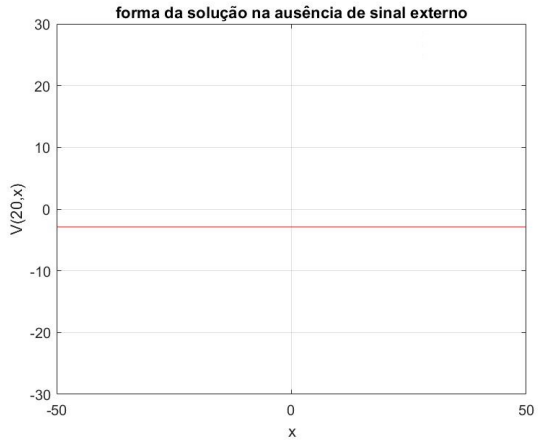

Figure 5: Shape of the solution in the absence of external stimulus $t = 20$

4.2. Solution with $\sigma = 3$

In Fig.6 the evolution of the solution in $x = 0$ is represented. It is clear that at instant $t = 10$, there is no longer any external stimulus. This time, we see a more significant increase in the solution compared to the previous result, so after decreasing, it stabilizes at a higher value. From the instant $t = 15$, the graph of the solution coincides with the one of the stationary solution, which in this case satisfies $V(0) = 10$ (see fig. 8).

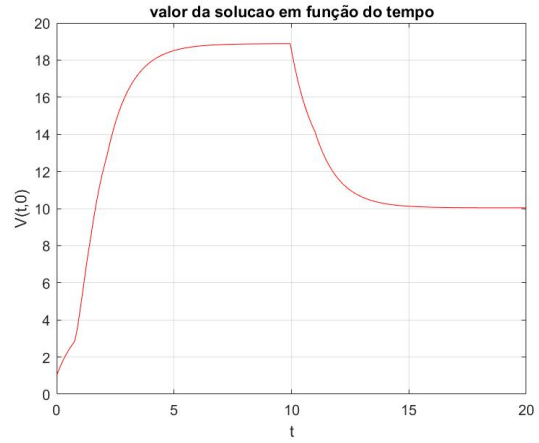

Figure 6: Solution in $x = 0$ in function of time in case of $\sigma = 3$

In Fig.7, the external signal function is represented in red and in blue, the solution in space for the instant $t = 10$. As we can see, the solution behaves similarly to the external signal as we saw earlier.

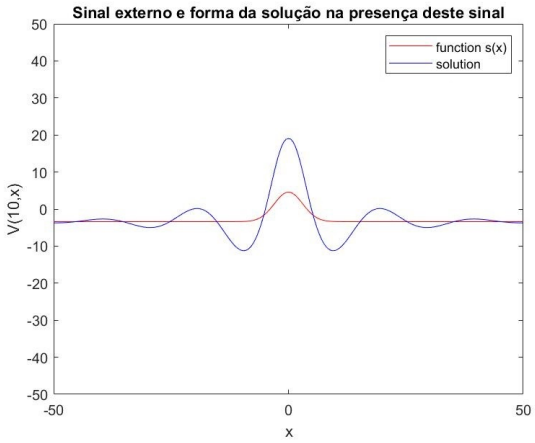

Figure 7: External stimulus and solution in $t = 10$ in case of $\sigma = 3$

Starting from this point, the behaviour of the solution is very different from what happens in the case $\sigma = 0.4$. In Fig.8 we see that the stimulus was strong enough to create a "memory effect" in the neurons, because in the following figure, the solution in $t = 20$ is not constant and resembles the external stimulus in form. But while the maximum of the external stimulus, reached at $x = 0$, is approximately 20, that of the stationary solution is approximately 10.

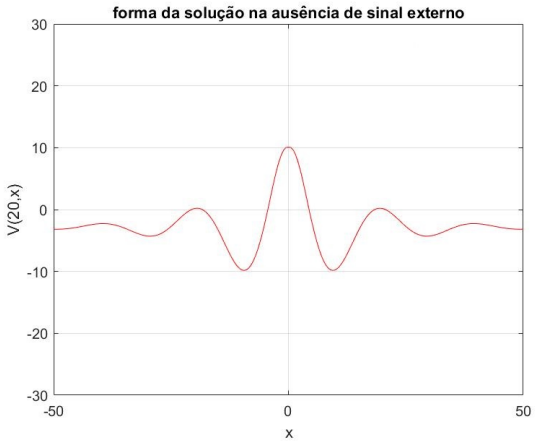

Figure 8: Shape of the solution in the absence of external stimulus $t = 20$

The observed results allow us to conclude about the existence of stationary solutions, whose shape depends on the shape of the external stimulus. First, the solution evolves into a new state, triggered by the external stimulation. After this is annulled, the evolution to the steady state is verified, which represents the memory effect. This only occurs if the stimulus is strong enough.

5. Conclusions

The study of the convergence of the three methods, explicit, semi-implicit and implicit, revealed first order of convergence with respect to time step size and second order, with respect to space step size. The conditions under which convergence is guaranteed are derived in Sec. 3. The higher computational cost of the implicit method, compared with the explicit one, is compensated by its greater stability. The comparative analysis of the three methods revealed the advantages of the implicit method in comparison with the explicit one, when the numerical solution of the NFE is considered. Throughout the examples presented, we observed in the tables that the implicit method presents the smallest error. The semi-implicit method did not always present smaller errors compared to the explicit one. The use of MatLab rises some limitations in terms of calculation time when we wanted a refined network. For future work, an approach with a more developed language, like Julia, for example, could bring some advantages in comparison with Matlab. The numerical experiments carried out in Chap. 4, when the NFE is solved in the case of a transient external signal, confirm that if the signal satisfies certain conditions, the stationary solution of the NFE may reflect its properties, namely, the existence of a bounded domain of neuronal activity (bump). Such stationary solutions reflect a phenomenon known as working memory. The numerical methods in the thesis can be adapted in order to take into account the delay effect, resulting from the fact that propagation speed is finite. In chapter 3 an example is described in which this delay is considered. For future research, we want to apply the delay equation to the study of real-life phenomena, such as working memory.

References

[1] Valerie Ross.: Numbers: The Nervous System, From 268-MPH Signals to Trillions of Synapses. Discover Magazine, May 15, 2011

[2] Hodgkin, A.L. and Huxley, A.F. A quantitative description of membrane current and its application to conduction and excitation in nerve. Bulletin of Mathematical Biology, 52(1):25 – 71, 1990. ISSN 0092-8240. doi: https://doi.org/10.1016/S0092-8240(05)80004-7.

[3] FitzHugh, Richard. Impulses and physiological states in theoretical models of nerve membrane. Biophysical Journal, 1(6):445 – 466, 1961. ISSN 0006-3495. doi: https://doi.org/10.1016/S0006-3495(61)86902-6. URL http://www.sciencedirect.com/science/article/pii/S0006349561869026.

[4] Fitzhugh, Richard. Computation of impulse initiation and saltatory conduction in a myelinated nerve fiber. Biophysical Journal, 2(1):11 – 21, 1962. ISSN 0006-3495. doi: https://doi.org/10.1016/S0006-3495(62)86837-4. URL http://www.sciencedirect.com/science/article/pii/S0006349562868374.

[5] Nagumo, J. and Arimoto, S. and Yoshizawa, S. An active pulse transmission line simulating nerve axon. Proceedings of the IRE, 50(10):2061–2070, Oct 1962. ISSN 0096-8390. doi: 10.1109/ JRPROC.1962.288235.

[6] Beurle, R.L. Properties of a mass of cells capable of regenerating pulses. Philosophical Transactions of the Royal Society of London. Series B, Biological Sciences, 240, 08 1956. doi: 10.1098/rstb.1956.0012.

[7] Griffith, J.S. A field theory of neural nets: I: Derivation of field equations. The Bulletin of mathematical biophysics, 25, 1963. doi: https://doi.org/10.1007/BF02477774.

[8] Griffith, J.S. A field theory of neural nets: Ii. properties of the field equations. The Bulletin of mathematical biophysics, 27:187–95, 07 1965. doi: 10.1007/BF02498774.

[9] Wilson, Hugh and Cowan, Jack. Excitatory and inhibitory interactions in localized populations of model neurons. Biophysical journal, 12:1–24, 02 (1972). doi: 10.1016/S0006-3495(72)86068-5.

[10] Amari, S. Dynamics of pattern formation in lateral-inhibition type neural fields. Biol. Cybern., 27 (1977). https://doi.org/10.1007/BF00337259.

[11] Faye, G., Faugeras, O.: Some theoretical and numerical results for delayed neural field equations. Physica D: Nonlinear Phenomena 239, 561-578, 2010.

[12] Daniele Avitabile, Stephen Coombes, Pedro M. Lima.:Numerical investigation of a neural field model including dendritic processing. Journal of Computational Dynamics, V.7 (2020), pp. 271-290

[13] P.M . Lima and E. Buckwar.: Numerical solution of the neural field equation in the two-dimensional case, SIAM Journal of Scientific Computing, 37 (2015) B962– B979.

[14] Flora Ferreira.: Multi-bump solutions in dynamic neural fields: analysis and applications, PhD thesis, University of Minho, 2014 (http://hdl.handle.net/1822/34416).